Characterization of an Optoelectronic Polymer, Poly(2-phenoxy *p*-phenylene vinylene), and its Precursor Polymer by Dynamic Infrared Spectroscopy

JAMES N. WILKING,* CHRISTOPHER J. MANNING, and GEORGIA A. ARBUCKLE-KEIL†

Department of Chemistry, Rutgers University, 315 Penn Street, Camden, New Jersey 08102 (J.N.W., G.A.A.-K.); and Manning Applied Technology, 419 South Main Street, Troy, Idaho 83871 (C.J.M.)

Numerous applications of dynamic infrared spectroscopy to study a variety of polymer systems have been described in the literature. Typically, dynamic spectral changes are used to determine the molecular and submolecular reorientations that give rise to a material's observable mechanical properties. In the present study, the normal modes are characterized by their time-dependent response to an applied perturbation as an aid to assignment of the observed vibrational bands. Characterization of a newly synthesized optoelectronic polymer, poly(2-phenoxy *p*-phenylene vinylene), and its precursor polymer, is described. Vibrational modes along the backbone and side chain are expected to exhibit significantly different responses to mechanical perturbation due to delayed phase response of the phenoxy substituent. In-phase spectra, quadrature spectra, and two-dimensional infrared correlation maps are included in this characterization. This study has demonstrated that dynamic infrared spectroscopy can be used to distinguish backbone phenylene ring stretches from ring stretches associated with the phenoxy substituent. Density functional theory calculations are applied to confirm infrared spectral assignments. The mechanical properties are briefly discussed in light of the dynamic response.

Index Headings: **Dynamic infrared spectroscopy; PO-PPV; Poly(2-phenoxy *p*-phenylene vinylene); PPV; Chlorine precursor route; Two-dimensional infrared spectroscopy; 2D-IR; Rheo-optics.**

INTRODUCTION

Step-scan Fourier transform infrared (FT-IR) spectroscopy is a powerful and versatile technique for recording spectra of time- and frequency-dependent phenomena.[1] The exploitation of this capability in phase-resolved experiments using mechanical sample modulation is discussed here. In addition to sample modulation, these experiments use phase modulation. Relatively recent advances in digital signal processing have eliminated the need for multiple lock-in amplifiers and have simplified the technique.[2–5] In dynamic infrared spectroscopy, an external periodic perturbation is applied to a system, resulting in a dynamic spectral response. The resulting molecular re-orientations are monitored via step-scan infrared spectroscopy. These re-orientations induce frequency shifts and/or changes in absorption intensity that make up the resulting dynamic spectra. The dynamic spectrum is composed of two orthogonal components, the in-phase and the quadrature signals, both of which can be isolated as individual interferograms and the corresponding spectra. This technique has been used to study numerous polymer systems including isotactic polypropylene (iPP),[6,7] polystyrene,[8] the degradation of poly(ester urethane),[9] and the secondary structure of silk fibroin film,[10] as well as others too numerous to mention.[1,11] The focus of this study is the characterization of a newly synthesized conjugated polymer and its precursor polymer by dynamic infrared spectroscopy. While this relatively new technique has many uses in polymer chemistry, little application has been made in the field of conjugated conducting polymers.[12]

Conjugated conducting polymers, also known as *synthetic metals* and more commonly *conducting polymers,* have attracted much interest for their high electrical conductivities[13] and optoelectronic properties.[14] Since the discovery of conductivity in doped polyacetylene in 1977,[15] much research has focused on the synthesis and development of these materials. Interest in these electroactive polymers was initially due to their electrical properties: intrinsic semi-conductivity and increased conductivity, by several orders of magnitude, upon doping. The focus of research shifted in 1990 when electroluminescence was first discovered in a conducting polymer, poly(*p*-phenylene vinylene) (PPV).[16] Since that discovery, PPVs have shown potential for application in organic light emitting diodes.[17] The ability to alter the bandgap and therefore the wavelength of emission by substituting electron-donating or -withdrawing substituents onto the PPV backbone has led to the synthesis of numerous PPV derivatives.[18] The unique properties of conducting polymers are due to their delocalized π-electron system. Unfortunately, conjugation also generally leads to insolubility and the resulting processing problems must be circumvented. The most common solution to the processing problem is the use of a soluble precursor,[19] which is the method used here. Insolubility is overcome by the development of soluble, processable precursor polymers that can be thermally converted into the final conjugated polymer.

The optoelectronic polymer of interest in this study is a newly synthesized PPV derivative, poly(2-phenoxy *p*-phenylene vinylene), referred to here as PO-PPV; further characterization of this yellow light-emitting polymer will be published elsewhere.[20] PO-PPV has been synthesized via the chlorine precursor route (CPR).[20,21] This route is useful for the synthesis of PPV derivatives with bulky side groups.[22] The thermal elimination reaction that converts the precursor polymer to PO-PPV is illustrated in Fig. 1. The vibrational spectra of both PO-PPV and its

Received 27 May 2003; accepted 4 November 2003.

* Present Address: Department of Chemistry and Biochemistry, Box 951569, UCLA, Los Angeles, CA 90095-1569.

† Author to whom correspondence should be sent. E-mail: arbuckle@camden.rutgers.edu.

0003-7028/04/5803-0304$2.00/0

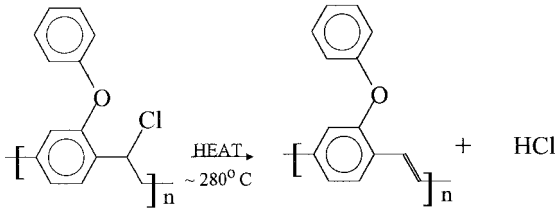

PO-PPV Precursor PO-PPV

FIG. 1. The thermal elimination reaction of the PO-PPV precursor converting to PO-PPV.

precursor polymer are characterized here by dynamic infrared spectroscopy; the data are analyzed as both phase and magnitude spectra and two-dimensional infrared (2D-IR) correlation plots. Spectral bands associated with side-group and backbone vibrations can be distinguished by the difference in their time-dependent response to mechanical perturbation. This approach is based on the following principle. Vibrational modes immediately affected by a perturbation appear in the dynamic in-phase spectrum. Modes less directly affected, such as those associated with side groups, generally experience a phase lag. Depending on the extent of the phase lag, these modes will appear with more or less intensity in the quadrature spectrum. The phase plot provides clear dynamic information wherever there is sufficient intensity for accurate calculation. The phase plot of modes responding in-phase will exhibit similar phase angle; vibrational modes with phase lag exhibit a phase shift. The magnitude plot provides a gauge of the intensity of response of each band to perturbation, but it should be noted that this information includes a factor from the parent band intensity. Even when the dynamic spectra are normalized by dividing by the single-beam transmission spectrum, the dependence of the dynamic spectral amplitude on the parent band strength (intensity) remains. The linkage arises because a perturbation of a strong band results in a larger signal than the same degree of perturbation of a weaker band. Thus, the magnitude of response for different bands cannot be directly compared without considering the parent band intensities. Two-dimensional correlation of the dynamic spectra yields synchronous and asynchronous plots. These data are complementary to the phase and magnitude spectra and are useful in providing enhanced spectral resolution.[6,23,24] Unfortunately, IR-active vibrations, especially in macromolecules, are never completely localized, and intermolecular interactions may affect the phase response of a particular vibration. These factors may result in a less easily predicted dynamic response. Density functional theory (DFT) calculations of the infrared spectra of both polymers were performed to support the assignment of infrared vibrational bands with the aid of dynamic infrared spectroscopy. A detailed discussion of these calculations will be published elsewhere.[20] The mechanical response of each polymer at fixed frequency and temperature was recorded during the spectroscopic experiment (i.e., *in situ*). These rheological data were compared with those obtained by dynamic mechanical analysis (*ex situ*) of the two polymers over a broad temperature range. The dynamic spectral response is discussed in light of the macroscopic mechanical properties.

EXPERIMENTAL

Sample Preparation. The precursor polymer of PO-PPV was synthesized by the polycondensation of 2-phenoxy-1,4-bis(chloromethyl)benzene.[20] Free-standing films of the PO-PPV precursor were cast on a teflon substrate from a 0.35 w/v % chloroform solution. Precursor films were drawn to four times their original length while heating with a hot-air gun. A draw ratio of 10:1 is achievable, but with increased risk of breakage. This treatment serves to orient the films, and therefore improves the amplitude of subsequently measured dynamic spectra.[25] Heating during the drawing process also aided in the removal of residual chloroform. PO-PPV films were obtained by heating the drawn PO-PPV precursor films under an inert atmosphere at 280 °C for 2 hours. Heating converts the PO-PPV precursor to its conjugated analogue by the reaction illustrated in Fig. 1. Unfortunately, the glass transition of the PO-PPV precursor is approximately 59 °C, and, as a result, orientation was lost upon conversion. This effect was demonstrated by comparing the dynamic spectra of PO-PPV films oriented before conversion with those of PO-PPV films that had not been oriented before conversion. The spectral features and intensities proved to be virtually indistinguishable. PO-PPV films are much less processable than the precursor, and a draw ratio of only 1.5/1 could be achieved after thermal conversion without breaking the film. Films of the PO-PPV precursor and PO-PPV were approximately 2.5 cm square and 10–20 μm thick. Reproducibility of the dynamic IR spectra was demonstrated; multiple polymer film samples were prepared because the film must be homogeneous and cohesive in order to withstand the physical perturbation.

Instrumentation. The experimental setup was similar to that described previously.[12] Dynamic strain was applied to the sample by a piezo-driven Polymer Modulator™ microrheometer (Manning Applied Technology, Moscow, ID). A sinusoidal signal produced by an Agilent 33120A Function Generator/Arbitrary Waveform Generator was used to drive the Polymer Modulator™ microrheometer. A stretching amplitude of 75 μm was applied, corresponding to a deformation of approximately 0.1%. The sample modulation frequency was 16 Hz for all measurements described here. All dynamic spectra were collected with a Bio-Rad FTS 6000 step-scan FT-IR spectrometer (Digilab USA, Randolph, MA) in step-scan mode. All static spectra were collected in the rapid-scan mode. A phase modulation frequency of 400 Hz, with an amplitude of $2\lambda_{HeNe}$ was used for all the step-scan measurements. A signal pulse (BSTEP) generated with each step of the moving mirror was used to trigger the function generator, thereby synchronizing the stretching waveform to the spectrometer step-scanning clock. A deuterated triglycine sulfate (DTGS) detector (Digilab) with a low-energy spectral limit of 400 cm^{-1} was used for both step-scan and rapid-scan measurements. A mercury cadmium telluride (MCT) detector was also used, but no additional spectral information was obtained. Therefore, the DTGS detector was routinely used. An undersampling ratio of 8 was used to provide a free spectral range of 1975 cm^{-1}. A wire grid polarizer (Digilab) allowed only radiation with an electric field oriented along the axis of dynamic

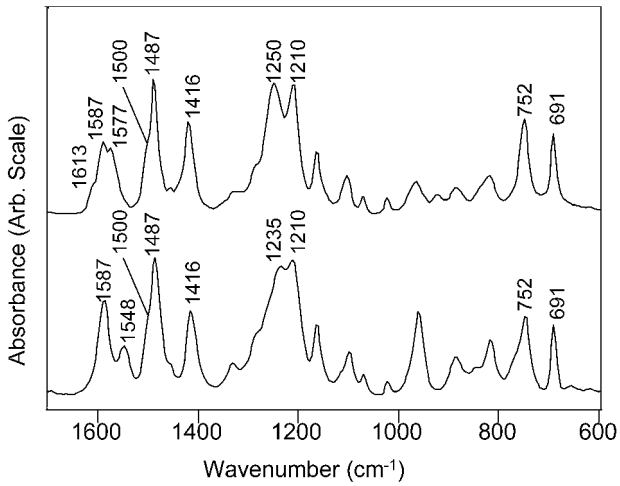

FIG. 2. Infrared absorbance spectra (1650–600 cm^{-1}) of (**top**) the PO-PPV precursor and (**bottom**) PO-PPV obtained in rapid-scan mode.

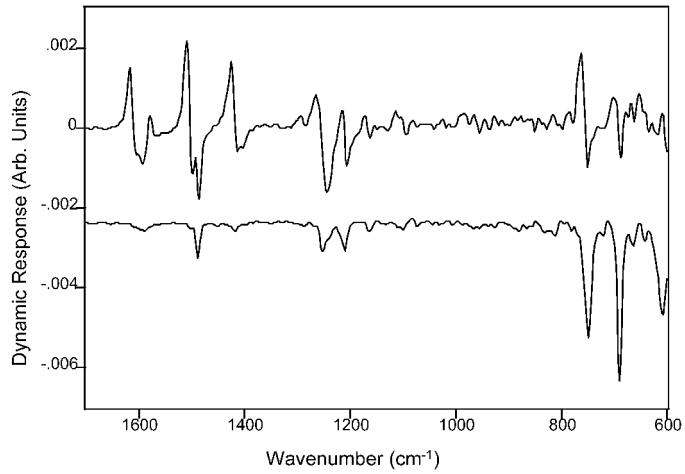

FIG. 3. (**Top**) Dynamic in-phase and (**bottom**) quadrature spectra (1650–600 cm^{-1}) of the PO-PPV precursor offset on the same scale.

stretching to reach the sample, and a low-pass optical filter (Digilab) was used to prevent aliasing.[26] Spectral resolution of 4 cm^{-1} was used for both static and dynamic spectral measurements. The dynamic spectra presented here are the average of three sequential scans, each requiring 40 minutes of acquisition time. Calibration of the electronic phase delay was performed with a partial beam block experiment.[27]

Rheological measurements at room temperature were derived from the stress and strain signals generated by the Polymer Modulator™ microrheometer. These signals were digitized and recorded using a data acquisition board (PC-5102, National Instruments, Austin, TX) in conjuction with VirtualBench™ (National Instruments), a computer oscilloscope program. The data were analyzed to extract rheological values using Matlab™ (Version 5.3, Mathworks, Inc., Natick, MA). Mechanical studies over a range of temperature, 25–140 °C, were performed using a dynamic mechanical analyzer (DMA) (Model 2980, TA Instruments, Newark, DE), equipped with a film tension clamp. The same modulation frequency, amplitude, and polymer samples were used for both dynamic infrared and DMA experiments to simplify comparison. Typical sample size was 12 mm × 7 mm × 0.02 mm. A heating rate of 1 °C/minute was used to minimize thermal lag.

Computational Details. Density functional theory calculations were used to model the infrared spectra of both PO-PPV and its precursor polymer.[20] A six-monomer ring was used to model an extended polymer chain in both cases. Structure optimization and frequency calculations were performed using Q-Chem 2.0,[28] an electronic structure program package. The Gauss View graphics package was used to visualize the results. For both calculations the B3LPY exchange-correlation functional and 3-21G basis set were used. Each spectrum took approximately one month to compute (Silicon Graphics Workstation, R12K Processor).

RESULTS AND DISCUSSION

Infrared Absorbance Spectra. The infrared absorbance spectra of the PO-PPV precursor and PO-PPV in the region 1700–600 cm^{-1} are shown together, offset, in Fig. 2. The band assignments for PPV are well established[29] and have proven beneficial in the identification of the vibrational spectra of PO-PPV and its precursor polymer. In the current study, three regions of the spectrum exhibit a strong dynamic response. These regions are primarily defined by the following vibrations: ring stretches (1650–1350 cm^{-1}), ether stretches (1300–1150 cm^{-1}), and phenoxy C–H out-of-plane bends (800–650 cm^{-1}). While these regions are not specific to these particular vibrations alone, they are the principal vibrational modes based on the structure of the polymers. Since thermal conversion of PO-PPV precursor to PO-PPV (as shown in Fig. 1) involves the loss of HCl and induced conjugation, the infrared spectral assignments given in Table I are similar for both polymers.

Dynamic Infrared Spectra: In-Phase and Quadrature. All dynamic infrared spectra, in-phase and quadrature, have been normalized against the single beam spectrum, yielding relative transmittance spectra. The dynamic infrared spectra of the oriented PO-PPV precursor are shown in Fig. 3. All dynamic spectra in this figure and the following figure are plotted on the same scale, but with an offset added for clarity. In general, the intensity of the quadrature spectra are less than those of the in-phase, with the exception of two vibrational bands at 752 and 691 cm^{-1}, which show a strong response in the

TABLE I. Band assignments of PO-PPV precursor and PO-PPV based on their dynamic response.

Assignment	PO-PPV Precursor (cm^{-1})	PO-PPV (cm^{-1})
C–C ring str. (origin unspecified[29])	1613(w), 1587(m), 1577(m)	1587(s), 1548(m)
C–C ring str. (backbone)	1500(m), 1416(s)	1500(m), 1416(s)
C–C ring str. (backbone & phenoxy)	1487(vs)	1487(vs)
C–O–C str.	1250(vs), 1210(vs)	1235(vs), 1210(vs)
Phenoxy C–H out-of-plane bend	752(s), 690(s)	750(s), 691(s)

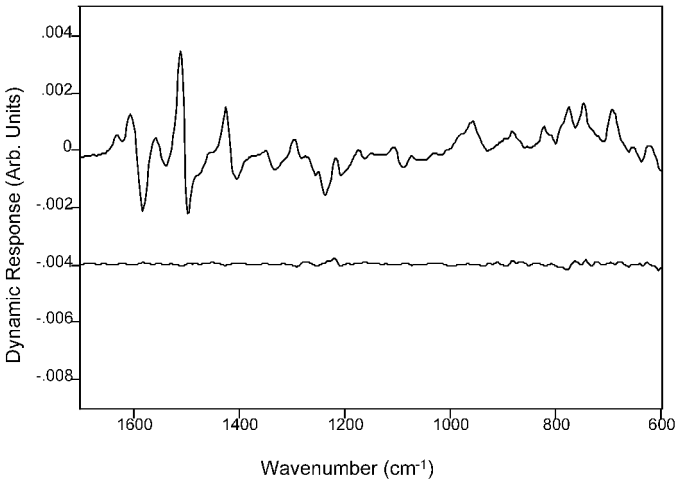

FIG. 4. (**Top**) Dynamic in-phase and (**bottom**) quadrature spectra (1650–600 cm^{-1}) of PO-PPV offset on the same scale.

quadrature spectrum. It has been established that bisignate, derivative-like peaks in a well-oriented sample are primarily due to strain-induced frequency shifts,[25] and monopolar peaks result primarily from spatial reorientations. Bisignate peaks commonly signify a strain-induced decrease in bond strength associated with a shift to lower wavenumber.[30]

The dynamic infrared spectra of PO-PPV are shown in Fig. 4. As described in the experimental section, a draw ratio of only 1.5/1 could be achieved with the PO-PPV films. This results in minimal orientation. Orientation along the polarization and stretching axis has been shown to result in a stronger in-phase signal. Despite lack of orientation, PO-PPV provides a stronger dynamic in-phase signal than the well-drawn precursor (Fig. 3). This is undoubtedly due to conjugation along the PO-PPV backbone, which results in an elastic and rigid polymer with a higher storage modulus and a stronger dynamic response than the relatively viscous PO-PPV precursor. The most definitive information can be obtained from the ring-stretch region of the PO-PPV dynamic spectra.

Ring Stretch Region, 1650–1350 cm $^{-1}$. The dynamic infrared spectra of the PO-PPV precursor prove useful in this region (Fig. 5a) by helping to distinguish ring stretches associated with the backbone from those associated with the phenoxy substituent. The infrared absorbance spectrum is also included in this figure. Bands at 1613, 1500, and 1416 cm^{-1} exhibit strong bisignate peaks in the in-phase spectrum. These bands show no significant quadrature response. Their presence as bisignate peaks in the in-phase spectrum indicates immediate strain-induced frequency shifts. It is interesting to note that peaks at 1613 and 1500 cm^{-1} are of low intensity in the absorbance spectrum relative to peaks at 1587, 1577, and 1487 cm^{-1}, yet they provide strong dynamic response. The disproportionately large perturbation indicates an association with the polymer backbone, supporting the subsequent assignment of these peaks as backbone phenylene ring stretches. These assignments are also supported by DFT calculations. Backbone phenylene rings in the dynamic spectrum of PPV have shown similar bisignate peaks.[12]

The ring stretch vibration at 1487 cm^{-1} is strongly supported by DFT calculations as a vibration involving phenylene rings in both the backbone and the side-group phenoxy. This assignment is supported by negative features in both the in-phase and quadrature spectra as shown in Fig. 5a. The negative feature at 1487 cm^{-1} in the in-phase spectrum is likely a negative monopolar peak, the negative component of a bipolar feature, or possibly a combination of the two. The negative monopolar band in the quadrature spectrum can be attributed to spatial reorientation of the phenoxy group. It is more difficult to identify the dynamic response of the IR bands at 1587 and 1577 cm^{-1} using only dynamic infrared spectra.

The dynamic (in-phase and quadrature) spectra, as well as the infrared absorbance spectra, of PO-PPV in the 1650–1350 cm^{-1} region are shown in Fig. 5b. Similar to its precursor, the in-phase spectrum of PO-PPV shows strong bisignate features centered over the backbone ring bands at 1500 and 1416 cm^{-1}. As in the precursor, these large perturbations indicate polymer backbone vibrations. The backbone ring-stretch vibrations are distinguished

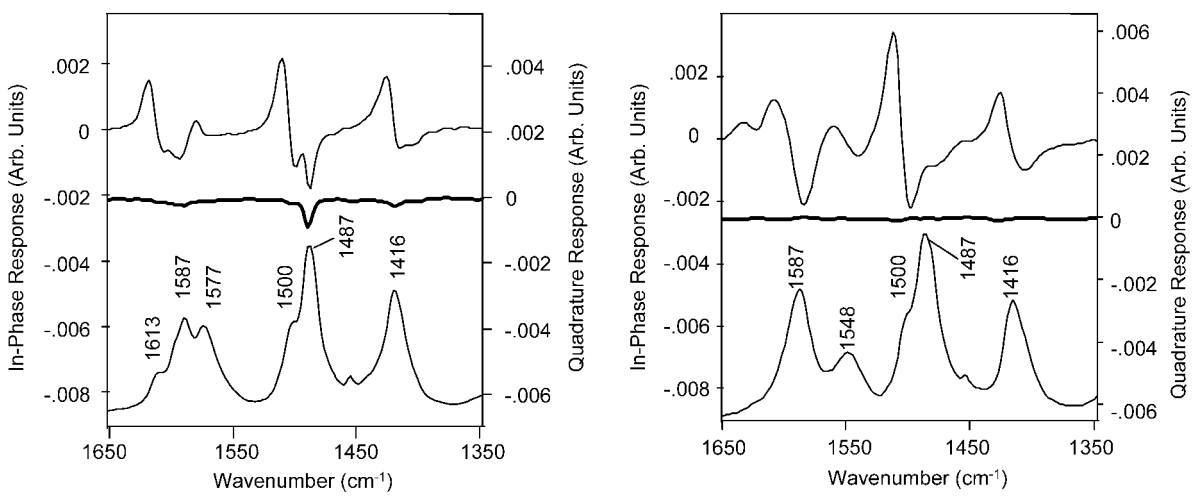

FIG. 5. (**Left**) Dynamic (in-phase (***top***) and quadrature (***middle,*** bold)) and absorbance spectra (***bottom***) (with peak labels) of the PO-PPV precursor in the ring stretch region, 1650–1350 cm^{-1}. (**Right**) Dynamic (in-phase (***top***) and quadrature (***middle,*** bold)) and absorbance spectra (***bottom***) (with peak labels) of PO-PPV in the ring stretch region, 1650–1350 cm^{-1}.

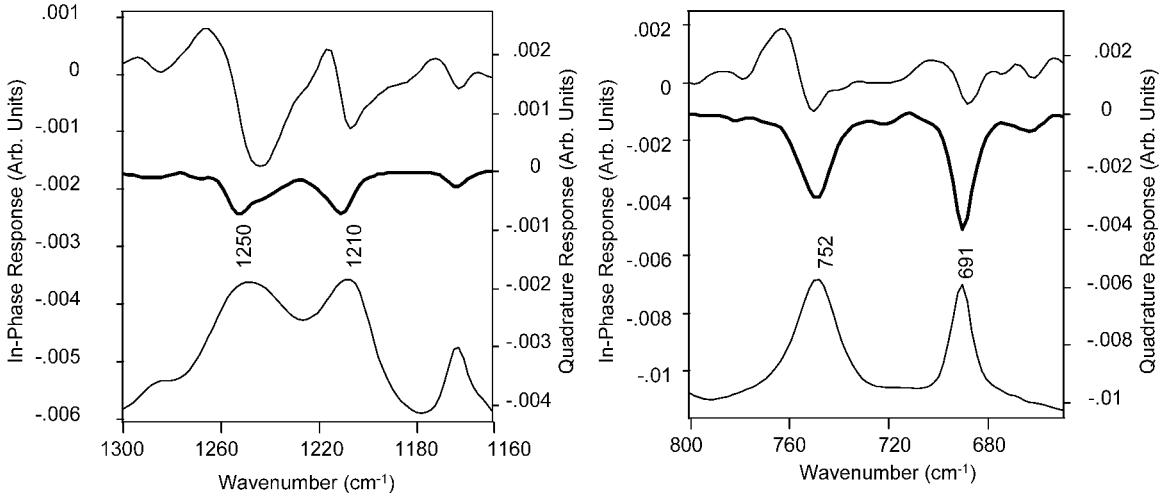

FIG. 6. (**Left**) Dynamic (in-phase (***top***) and quadrature (***middle,*** bold)) and absorbance spectra (***bottom***) (with peak labels) of the PO-PPV precursor in the ether stretch region, 1300–1160 cm^{-1}. (**Right**) Dynamic (in-phase (***top***) and quadrature (***middle,*** bold)) and absorbance spectra (***bottom***) (with peak labels) of PO-PPV precursor in the phenoxy C–H out-of-plane bend region, 800–650 cm^{-1}.

from the ring-stretch vibrations associated with the phenoxy substituent. A vibration at 1548 cm^{-1}, which is not present in the absorbance spectrum of the PO-PPV precursor (Fig. 5a), exhibits a strong dynamic response in the in-phase spectrum of PO-PPV. Additionally, the peak at 1587 cm^{-1}, which is present in the absorbance spectra of both polymers, exhibits a stronger dynamic response in the in-phase spectrum of PO-PPV. Peaks at 1613 and 1577 cm^{-1} in the absorbance spectrum of the PO-PPV precursor do not appear in the absorbance or dynamic spectra of PO-PPV, as also noted in Table I.

Ether Stretch Region, 1300–1160 cm $^{-1}$. While PPV lacks any strong characteristic vibrations in this region,[29] this is an area of intense absorption for both the PO-PPV precursor and PO-PPV (Fig. 2). This broad infrared absorbance is in the expected region for aryl ether asymmetric and symmetric stretches.[31] This is also a region for in-plane C–H deformation vibrations (1290–1000 cm^{-1}), but their intensity is expected to be medium to weak, and no dynamic response has been seen in the study of PPV.[12] The dynamic (in-phase and quadrature) spectra and static absorbance spectra for the PO-PPV precursor in this region are shown in Fig. 6a. Two absorption peaks, at 1250 and 1210 cm^{-1}, exhibit a strong dynamic response with a definite phase lag. Each exhibits a bisignate peak in the in-phase spectrum and a negative monopolar peak in the quadrature spectrum. The vibration at 1250 cm^{-1} shows a stronger in-phase response. Both bisignate features in the in-phase have a predominantly negative component. The unsymmetrical nature of these features indicates two combined effects: strain-induced frequency shifts and spatial reorientations. The intense component is a result of strain-induced reorientation of the ether dipole axis. The phase lag of these vibrations is evidenced by the monopolar bands in the quadrature spectrum. These are due solely to the delayed reorientation of the ether dipole axis.

No definitive information can be obtained from the dynamic spectra of PO-PPV in this region. However, by comparing the infrared absorbance spectra of the PO-PPV precursor and PO-PPV (Fig. 2), it can be seen that the ether stretch at 1250 cm^{-1} shifts to 1235 cm^{-1}. This indicates a susceptibility of the vibrational frequency to changes in the electronic environment along the polymer backbone (i.e., conjugation resulting from loss of HCl). The susceptibility of this vibration, combined with the predominantly in-phase response (Fig. 6a) indicates that this ether stretch is strongly associated with the backbone. DFT calculations also indicate that the higher energy stretch is slightly localized on the ether linkage to the backbone phenyl moiety.

Phenoxy C–H Out-of-Plane Bend Region, 800–650 cm $^{-1}$. The dynamic and infrared absorbance spectra for the PO-PPV precursor in this region are shown in Fig. 6b. The absorption bands in this region are characteristic of out-of-plane C–H and ring deformations for a 1,2,4-trisubstituted benzene and the phenoxy group. No significant vibrational modes appear in this region of the absorbance spectrum of PPV. Based on literature values and supporting DFT assignments, two predominant peaks at 752 and 691 cm^{-1} can be confidently identified as combination phenoxy out-of-plane C–H and ring deformations.[31] This assignment is supported by an unusually strong dynamic response, as monopolar bands, in the quadrature spectrum (Fig. 6b). The unusually strong response indicates that the primary dipole axes are reorienting with a definite phase lag. Both peaks exhibit a bisignate response in the in-phase spectrum. This immediate response is not surprising considering that strong π–π interactions between the phenoxy ring and the aromatic rings of neighboring chains are likely.

Phase and Magnitude Spectra. Phase and magnitude spectra provide an alternate representation of the information contained in the in-phase and quadrature spectra, as do the 2D-IR correlation maps discussed in the following section. The computation of both phase and magnitude spectra has been described in the literature.[32] Due to the similar structural nature of PO-PPV precursor and PO-PPV, spectral assignments are based primarily on the response observed from the well-oriented PO-PPV precursor. The phase and magnitude spectra of the well-oriented PO-PPV precursor were analyzed.

The phase spectrum (not shown) in the region of the backbone ring vibrations at 1613, 1500, and 1416 cm^{-1} in the PO-PPV precursor exhibits an abrupt phase shift over each bisignate band. These sharp changes may be indicative of quadrant boundary crossings, where the sign of either the in-phase or quadrature component changes. The two portions of the bisignate band, on either side of the boundary crossing, have very similar phase values. However, the arctangent function used to compute the phase must have at least one point in every 180° where the result changes sign abruptly. The phase spectra are similar for all three backbone vibrations, indicating an immediate and simultaneous response to the applied perturbation. A large phase shift was also observed for PPV[12] in this region. Further investigations into the significance and nature of this type of phase shift in conjugated polymers are in progress.

The ether stretches at 1250 and 1210 cm^{-1} exhibit a phase lag across the bisignate feature. The similar phase shift of the 1250 cm^{-1} vibration to the 1613 and 1500 cm^{-1} backbone ring vibrations is in agreement with the DFT calculation, indicating that this vibration is localized on the ether linkage to the polymer backbone. The phase of the 1210 cm^{-1} vibration exhibits a slightly different phase response than the 1250 cm^{-1} vibration or the backbone ring modes; this is expected for side-group vibrational modes and is in agreement with calculations that indicate that this ether stretch is slightly localized on the phenoxy substituent. In addition, the gradual phase shift between the bisignate components indicates that multiple microstructural environments may be present.[12]

The phenoxy out-of-plane C–H and ring deformations at 752 and 691 cm^{-1} are characterized by a definite phase lag quite distinct from any of the other vibrations. These stretches experience a much greater phase lag than the ring and ether vibrations, as is evident from the quadrature spectrum in Fig. 6b and found in the phase spectrum.

Two-Dimensional Infrared Correlation Maps. Information provided by 2D-IR correlation maps is complementary to that obtained from phase and magnitude spectra. Synchronous 2D-IR maps enhance correlations between vibrational bands that are simultaneously varying. Asynchronous 2D-IR maps enhance correlations between IR bands whose intensities are fluctuating out of phase with one another. In the asynchronous map, the sign of the cross peak essentially indicates when one vibration is reorienting with respect to another. Asynchronous 2D-IR maps are beneficial in this study in highlighting reorientation differences between the general regions of the spectrum and in separating broad overlapping peaks.

The asynchronous spectrum for the 1650–600 cm^{-1} region is shown in Fig. 7. This map also indicates different reorientation rates for the various molecular components that were indicated by the phase and magnitude data. Most apparent are the strong cross peaks between the phenoxy vibrations at 752 and 691 cm^{-1} and the rest of the spectrum, particularly the backbone phenylene stretches, which indicates that these peaks are moving out of phase with the rest of the molecule. The ether stretches at 1250 and 1210 cm^{-1}, which are considered to have an intermediate phase lag, form cross peaks with the phenoxy vibrations at 752 and 691 cm^{-1}, but only weak

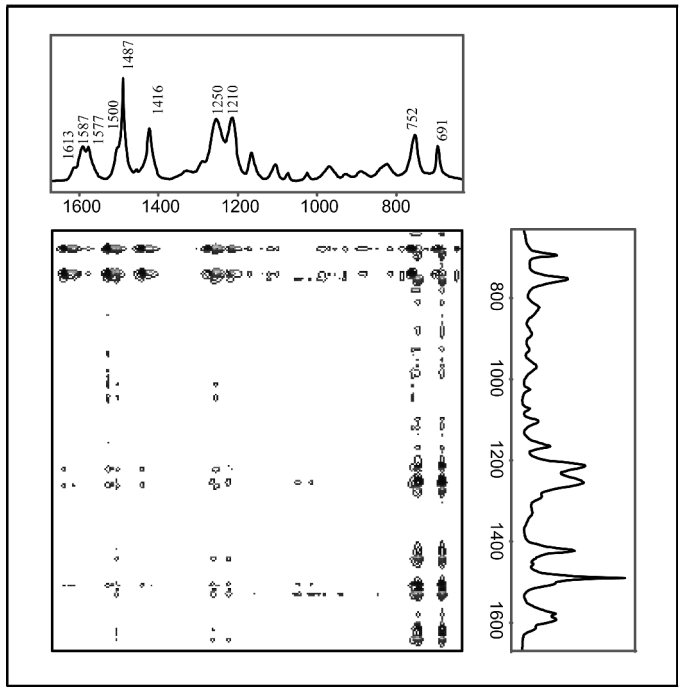

FIG. 7. Asynchronous 2D-IR of the PO-PPV precursor in the 1650–600 cm^{-1} region.

crosspeaks with the backbone phenylene ring stretches. The ether stretches are reorienting nearly synchronously with the backbone phenylene region, with only a slight phase lag. The asynchronous map indicates that the backbone ring stretches, ether stretches, and phenoxy stretches are all experiencing different phase responses.

Asynchronous correlation maps can be useful in distinguishing the number of different components within a band. This is beneficial in revealing overlapping bands and multiple microstructural environments. The phase and magnitude spectra indicate multiple microstructural environments in the case of the ether stretches at 1250 and 1210 cm^{-1} and the phenoxy vibrations at 752 and 691 cm^{-1}. The synchronous and asynchronous 2D-IR maps of the ether stretch region in the chlorine precursor are shown in Figs. 8 and 9. In the synchronous map (Fig. 8), three autopeaks along the diagonal are most apparent. An additional autopeak corresponding to the weak positive component of the 1210 cm^{-1} vibration is not visible in this figure. In this case, the asynchronous correlation map provides enhanced spectral resolution. As can be seen in Fig. 9, the peak at 1250 cm^{-1} is resolved into at least three correlation peaks. This supports the possibility of multiple microstructural environments. Due to low intensity, additional features of the peak at 1210 cm^{-1} are not seen.

Similar results can be observed in the synchronous and asynchronous 2D-IR maps in the 800–600 cm^{-1} region (Figs. 10 and 11). Autopeaks along the diagonal in the synchronous plot are expected, as peaks 752 and 691 cm^{-1} are moving in-phase with one another. The asynchronous plot reveals a number of additional cross peaks, also supporting the possibility of microstructural environments.

Rheological Measurements. Rheological measurements were obtained on both polymers in order to cor-

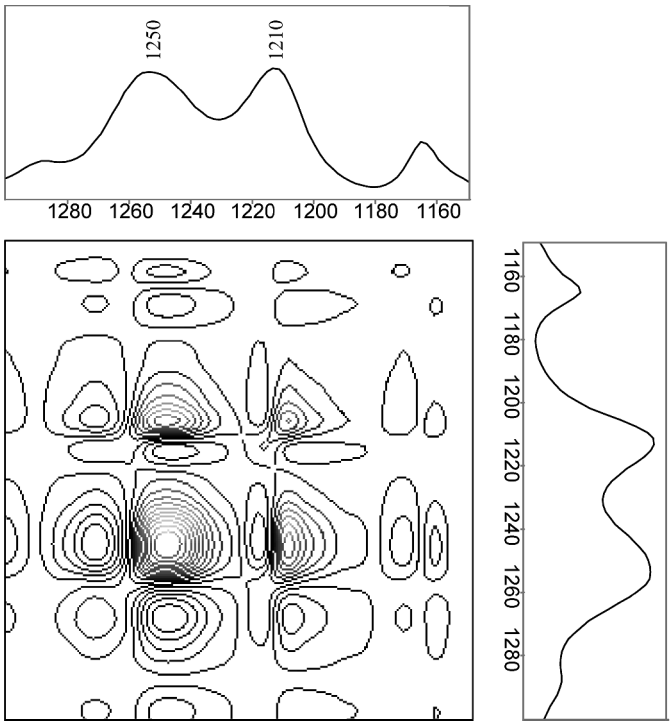

FIG. 8. Synchronous 2D-IR of the PO-PPV precursor in the ether stretch region, 1300–1150 cm^{-1}.

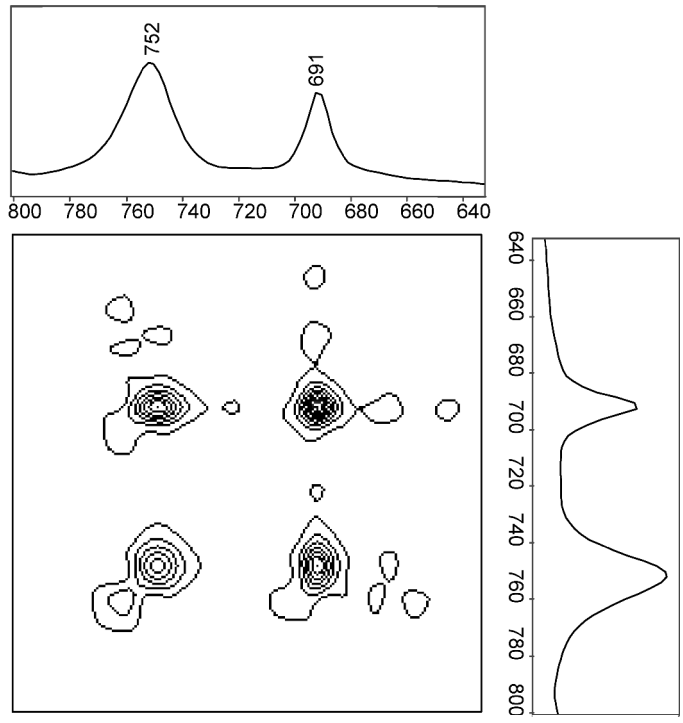

FIG. 10. Synchronous 2D-IR of the PO-PPV precursor in the phenoxy C–H out-of-plane bend region, 800–600 cm^{-1}.

relate the macroscopic behavior with the dynamic infrared analysis. The mechanical analysis was obtained by two different methods, both providing similar results. Stress and strain outputs from the Polymer Modulator™ microrheometer allowed measurements to be made *in situ*. Supporting measurements were made using a dynamic mechanical analyzer (*ex situ*). Both methods provided consistent results. The storage modulus (E′) and loss modulus (E″) of PO-PPV and the PO-PPV precursor from 25–130 °C, obtained by the *ex situ* method, are plotted in Fig. 12. As expected, the conjugated backbone of PO-PPV results in a higher storage modulus and lower loss modulus at room temperature than the PO-PPV precursor. The storage modulus of PO-PPV at room temperature (~2.4 GPa) is comparable to that reported for

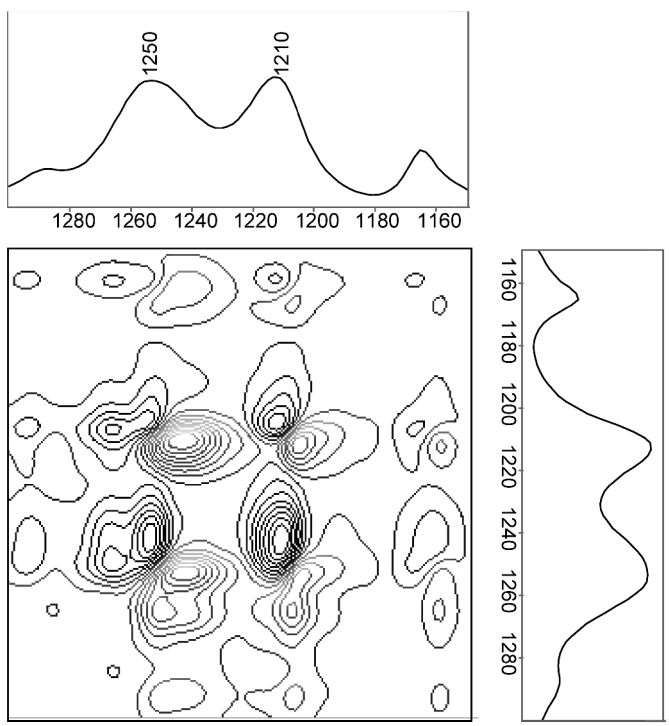

FIG. 9. Asynchronous 2D-IR of the PO-PPV precursor in the ether stretch region, 1300–1150 cm^{-1}.

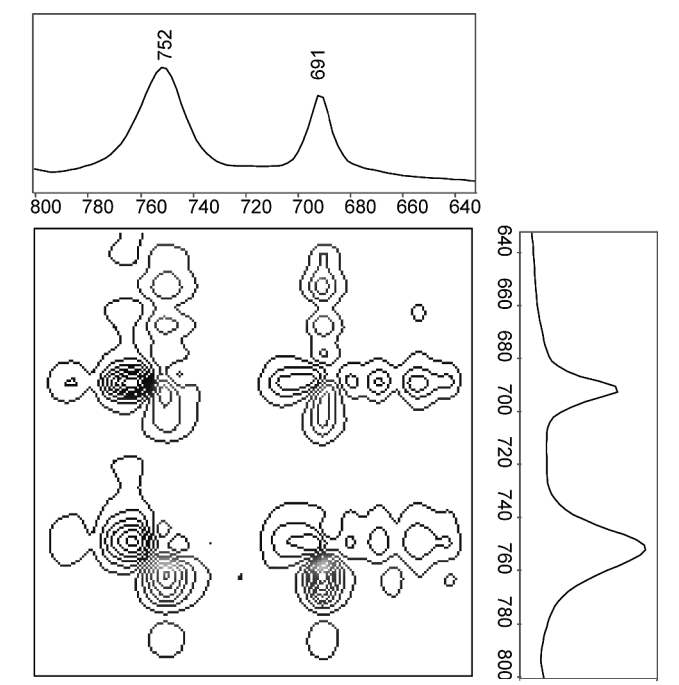

FIG. 11. Asynchronous 2D-IR of the PO-PPV precursor in the phenoxy C–H out-of-plane bend region, 800–600 cm^{-1}.

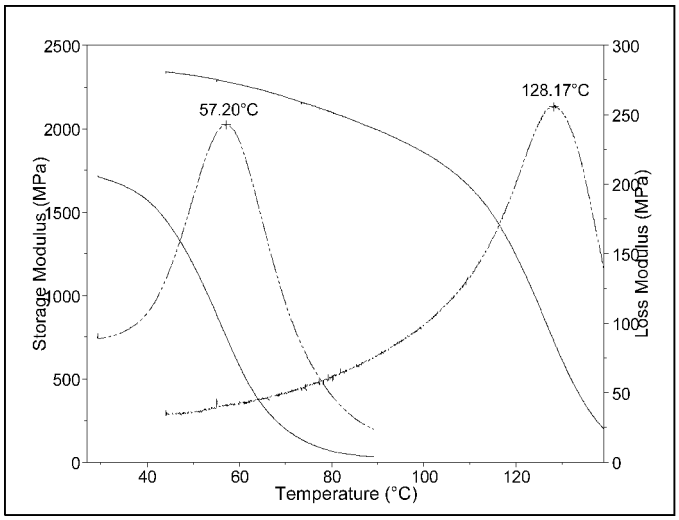

FIG. 12. The storage (solid) and loss (dashed) modulus of PO-PPV (both right) and the PO-PPV precursor (both left) over the temperature range 25–140 °C.

polyaniline (~2.5 GPa)[33] and higher than that of PPV (~1.8 GPa)[34] and polypyrrole (~0.5 GPa).[35] The tan δ (not plotted) is a common measure of polymer viscoelasticity and is calculated as the ratio of the loss modulus and storage modulus (E″/E′). Tan δ values for PO-PPV and the PO-PPV precursor at room temperature are 0.02 and 0.06 radians, respectively. A higher tan δ value, as in the case of the chlorine precursor, indicates a larger phase angle, δ, and a more viscous response.

The phase angle, δ, between the stress and the strain waveforms was also measured *in situ* with the microrheometer during the dynamic IR measurement. This parameter was calculated for both PO-PPV and the PO-PPV precursor, and the corresponding tan δ values were compared with the *ex situ* results. As mentioned previously, the Matlab™ program was used to perform the following calculations on the recorded stress and strain signals. The application of the Fourier transform to both signals yielded real and imaginary components for each. The phase of both signals was calculated from the arctangent of the ratio of the real and imaginary components. The phase difference was calculated by subtraction of the two phase values at the stretching frequency. Phase angles obtained by this method contain an instrumental phase delay contribution. The ~0.04 radian difference observed between the tan δ values of PO-PPV and the PO-PPV precursor (*in situ*) supports the mechanical response observed by dynamic mechanical analysis (*ex situ*). A greater tan δ was found for the PO-PPV precursor than PO-PPV, indicating a greater phase lag (i.e., a more viscous response to the applied perturbation).

The macroscopic behavior described here (*ex situ* and *in situ*) also corresponds with the dynamic infrared results. As mentioned previously, a high degree of orientation was necessary in the PO-PPV precursor films before a strong dynamic infrared response could be obtained. The PO-PPV films exhibited a stronger dynamic infrared response than the precursor, despite lack of orientation. The particularly intense in-phase response of PO-PPV in the ring stretch region tends to indicate that the increase in elasticity (i.e., rigidity) is due primarily to conjugation along the backbone. The lack of a quadrature response in the PO-PPV may indicate that the substituent is responding instantaneously to the applied perturbation or may not be observable because of the low degree of orientation.

CONCLUSION

Dynamic infrared spectroscopy has been used to characterize PO-PPV and the PO-PPV precursor. The processable PO-PPV precursor, which can easily be oriented, yielded the most informative dynamic results. In-phase and quadrature spectra, phase and magnitude spectra, and 2D-IR correlation maps all provide similar information regarding the dynamic response. Vibrational modes have been seen to exhibit dynamic responses indicative of their location within the molecule. This has aided assignment of the absorbance spectra (Table I). The identification of a number of bands is supported by DFT calculations. Only slight spectral changes occur during thermal conversion from the PO-PPV precursor to PO-PPV. As a result, much of the characterization of the PO-PPV precursor can be applied to the absorption spectrum of PO-PPV. It has also been seen that vibrations associated with the phenoxy substituent, ether stretches, and out-of-plane C–H and ring deformations are more susceptible to differences in microstructural environments. The dynamic response of PO-PPV and the PO-PPV precursor are consistent with their observed macroscopic behavior. The desirable mechanical properties of optoelectronic PO-PPV and the PO-PPV precursor may lead to a variety of applications for this recently characterized polymer.

ACKNOWLEDGMENTS

This work was supported by NSF-ARI (CHE 96-01710) and NSF-RUI (DMR 00-75820). The authors thank Dr. Bing Hsieh for the synthesis and provision of the PO-PPV precursor polymer and Dr. Paul Maslen for the DFT calculations. Significant comments by the referees are appreciated.

1. E. Y. Jiang, Spectroscopy **17,** 22 (2002).
2. C. J. Manning and P. R. Griffiths, Appl. Spectrosc. **47,** 1345 (1993).
3. R. Curbelo, U. S. Patent 5,612,784 (2000).
4. R. Curbelo, U. S. Patent 5,835,213 (1998).
5. C. J. Manning, G. L. Pariente, B. D. Lerner, J. H. Perkins, R. S. Jackson, and P. R. Griffiths, in *Computer Enhanced Analytical Spectroscopy,* S. D. Brown, Ed. (John Wiley and Sons, New York, 1996), vol. 6, p. 1.
6. R. A. Palmer, C. J. Manning, J. L. Chao, I. Noda, A. E. Dowrey, and C. Marcott, Appl. Spectrosc. **45,** 12 (1991).
7. I. Noda, Appl. Spectrosc. **44,** 550 (1990).
8. C. Marcott, A. E. Dowrey, and I. Noda, Appl. Spectrosc. **47,** 1324 (1993).
9. J. R. Schoonover, D. G. Thompson, J. C. Osborn, E. B. Orler, D. A. Wrobleski, A. L. Marsh, H. Wang, and R. A. Palmer, Polymer Degrad. Stability **74,** 87 (2001).
10. M. Sonoyama and T. Nakano, Appl. Spectrosc. **54,** 968 (2000).
11. J. K. Gille, J. Hochowski, and G. A. Arbuckle-Keil, Anal. Chem. **72**(12), 71 (2000).
12. H. V. Shah, C. J. Manning, and G. A. Arbuckle, Appl. Spectrosc. **53,** 1542 (1999).
13. T. Ohnishi, T. Noguchi, T. Nakano, M. Hirooka, and I. Murase, Synth. Met. **41,** 309 (1991).
14. R. H. Friend, R. W. Gymer, A. B. Holmes, J. H. Burroughes, R. N. Marks, C. Taliani, D. D. C. Bradley, D. A. Dos Santos, J.-L. Bredas, M. Logdlund, and W. R. Salaneck, Nature (London) **397,** 121 (1999).
15. C. K. Chiang, C. R. Fincher, Jr., Y. W. Park, A. J. Heeger, H.

Shirakawa, E. J. Louis, S. C. Gau, and A. G. MacDiarmid, Phys. Rev. Lett. **39,** 1098 (1977).
16. J. H. Burroughes, D. D. C. Bradley, A. R. Brown, R. N. Marks, K. D. Mackay, R. H. Friend, P. L. Burn, and A. B. Holmes, Nature (London) **347,** 539 (1990).
17. R. H. Friend and N. C. Greenham, ''Electroluminescence in Conjugated Polymers'', in *Handbook of Conducting Polymers,* T. A. Skotheim, R. L. Elsenbaumer, and R. J. Reynolds, Eds. (Marcel Dekker, Inc., New York, 1998), Chap. 29, p. 823.
18. S. C. Moratti, ''The Chemistry and Uses of Polyphenylenevinylenes'', in *Handbook of Conducting Polymers,* T. A. Skotheim, R. L. Elsenbaumer, and R. J. Reynolds, Eds. (Marcel Dekker, Inc., New York, 1998), Chap. 13, p. 343.
19. D. L. Wise, G. E. Wnek, D. J. Trantolo, T. M. Cooper, and J. D. Gresser, *Photonic Polymer Systems: Fundamentals, Methods, and Applications* (Marcel Dekker, Inc., New York, 1998).
20. J. N. Wilking, G. A. Arbuckle-Keil, H. R. Kricheldorf, P. Maslen, and B. Hsieh, Macromolecules, paper to be submitted.
21. J. Wilking, G. Arbuckle-Keil, and B. Hsieh, The Rutgers Scholar **3** (2001), http://rutgersscholar.rutgers.edu/volume03/wilkarbu/wilkarbu.htm.
22. W. C. Wan, H. Antoniadis, V. E. Choong, H. Razafitrimo, Y. Gao, W. A. Feld, and B. R. Hsieh, Macromolecules **30,** 6567 (1997).
23. I. Noda, A. E. Dowrey, and C. Marcott, Appl. Spectrosc. **47,** 1317 (1993).
24. I. Noda, Appl. Spectrosc. **47,** 1329 (1993).
25. M. Sonoyama, K. Shoda, G. Katagiri, and H. Ishida, Appl. Spectrosc. **51,** 346 (1997).
26. C. Manning, *Polymer Modulator* (Manning Applied Technology, Moscow, Idaho, 2000), Version 2.1.
27. I. Noda, A. E. Dowrey, and C. Marcott, Appl. Spectrosc. **42,** 203 (1988).
28. J. Kong, C. A. White, A. I. Krylov, D. Sherrill, R. D. Adamson, T. R. Furlani, M. S. Lee, A. M. Lee, S. R. Gwaltney, T. R. Adams, C. Ochsenfeld, A. T. B. Gilbert, G. S. Kedziora, V. A. Rassolov, D. R. Maurice, N. Nair, Y. Shao, N. A. Besley, P. E. Maslen, J. P. Dombroski, H. Daschel, W. Zhang, P. P. Korambath, J. Baker, E. F. C. Byrd, T. Van Voorhis, M. Oumi, S. Hirata, C.-P. Hsu, N. Ishikawa, J. Florian, A. Warshel, B. G. Johnson, P. M. W. Gill, M. Head-Gordon, and J. A. Pople, J. Comp. Chem. **21,** 1532 (2000).
29. D. D. C. Bradley, J. Phys. D: Appl. Phys. **20,** 1389 (1987).
30. H. Wang, R. A. Palmer, and C. J. Manning, Appl. Spectrosc. **51,** 1245 (1997).
31. G. Socrates, *Infrared Characteristic Group Frequencies* (John Wiley and Sons, West Sussex, England, 1994), 2nd ed.
32. B. O. Budevska, C. J. Manning, and P. R. Griffiths, Appl. Spectrosc. **48,** 1556 (1994).
33. H. Okuzaki, T. Kira, and T. Kunugi, J. Appl. Polym. Sci. **75,** 566 (2000).
34. H. Okuzaki, Y. Hirata, and T. Kunugi, Polymer **40,** 2625 (1999).
35. T. Kunugi and H. Okuzaki, J. Polym. Sci.: Part B **34,** 1269 (1996).